RESEARCH ARTICLE

Evaluation of the wind direction uncertainty and its impact on wake modeling at the Horns Rev offshore wind farm

M. Gaumond[1], P.-E. Réthoré[1], S. Ott[1], A. Peña[1], A. Bechmann[1] and K. S. Hansen[2]

[1] DTU Wind Energy, Risø Campus, Roskilde, Denmark
[2] Department of Mechanical Engineering, Technical University of Denmark, Kgs Lyngby, Denmark

ABSTRACT

Accurately quantifying wind turbine wakes is a key aspect of wind farm economics in large wind farms. This paper introduces a new simulation post-processing method to address the wind direction uncertainty present in the measurements of the Horns Rev offshore wind farm. This new technique replaces the traditional simulations performed with the 10 min average wind direction by a weighted average of several simulations covering a wide span of directions. The weights are based on a normal distribution to account for the uncertainty from the yaw misalignment of the reference turbine, the spatial variability of the wind direction inside the wind farm and the variability of the wind direction within the averaging period. The results show that the technique corrects the predictions of the models when the simulations and data are averaged over narrow wind direction sectors. In addition, the agreement of the shape of the power deficit in a single wake situation is improved. The robustness of the method is verified using the Jensen model, the Larsen model and Fuga, which are three different engineering wake models. The results indicate that the discrepancies between the traditional numerical simulations and power production data for narrow wind direction sectors are not caused by an inherent inaccuracy of the current wake models, but rather by the large wind direction uncertainty included in the dataset. The technique can potentially improve wind farm control algorithms and layout optimization because both applications require accurate wake predictions for narrow wind direction sectors. Copyright © 2013 John Wiley & Sons, Ltd.

1. INTRODUCTION

The rising demand for wind power together with social, environmental and economical constraints currently lead to an increase in the size of wind turbines and wind farms. A drawback from installing wind turbines in large arrays is the wake penalty that arises when a wind turbine operates in the lee of another. In large offshore wind farms, the average energy loss due to wind turbine wakes is approximately 10% to 20% of the annual energy production.[1] As the wind flows through the rotors, turbulent structures are generated and transported downstream. The resulting turbulent velocity field reduces the wind turbine lifespan and increases maintenance costs. Therefore, it is crucial for wind farm developers to estimate accurately the impact of wind turbine wakes because it has become significant for wind farm economics.

Most engineering wake models currently used by the wind industry are still based on the classical work from Jensen,[2] Katic *et al.*[3] and Ainslie[4] in the 1980s, although the challenges of wake modeling have drastically changed since then. Today, wind farms are increasingly being installed in sites where the assumptions underlying these models are not valid. The characteristics of such sites include complex orography, forests and non-neutral atmospheric stability. The size of wind farms has also become an increasing issue because the engineering models tend to underestimate wake losses in large wind farms.[1,5,6] Some studies suggest that these deviations occur because wind power plants are now so large that they have an impact on the local boundary layer.[7,8]
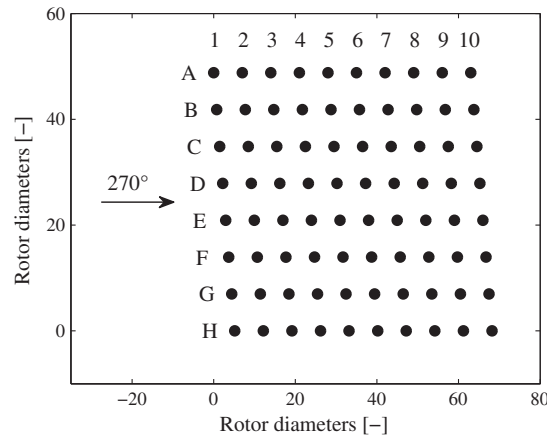
Figure 1. Layout of the Horns Rev offshore wind farm.

With the increase in computer power, several new wake models have been developed in an attempt to overcome these issues.[9] Some promising approaches include computational fluid dynamics methods using Reynolds-averaged Navier–Stokes (RANS) models[10,11] or large eddy simulations.[12–15] Nevertheless, several studies found that conventional RANS simulations overpredict the velocity inside the wakes due to the limitations of the Boussinesq hypothesis.[16–19]

The wide variety of available wake models emphasizes the need for additional validation campaigns to define clear guidelines on how the wind industry shall use the models.[20] A better understanding of the wake models' limitations will decrease wake loss uncertainty in project development and improve the competitiveness of wind energy. However, comparing numerical simulations with wind farm production data is a task that must be carried out carefully in a context where robust solutions are desired. Barthelmie *et al.*[1] underlined several aspects to consider when performing benchmarking studies with experimental data. One issue is the wind direction uncertainty included in the datasets because numerical simulations are very sensitive to a change of wind direction input.[21] In some cases, the reference wind direction of a whole wind farm is determined from the yaw position sensor of an upstream wind turbine during data processing. Hansen *et al.*[22] mentioned that this method 'results in an uncertainty of more than 7° because the yaw misalignment of the reference turbine also needs to be included'. In addition, spatial variability and time averaging of the wind direction increase the direction uncertainty in large wind farms due to the stochastic behavior of the wind. Gaumond *et al.*[23] suggested that the discrepancies of numerical simulations for narrow wind direction sectors (< 10°) found in previous studies[10,12,24] are not caused by wake modeling inaccuracies, but rather by the large wind direction uncertainty included in the datasets. Further, Gaumond *et al.*[23] highlighted a correlation between the width of the wind direction sector used for data binning and the agreement of the numerical simulations with wind farm data. It has become critical to quantify this uncertainty to enable a better and fairer comparison between numerical simulations and power production data. Ultimately, the robustness of the models should improve by excluding the site-specific dataset uncertainty from the model calibrations.

This paper proposes in Section 3 a new method to address the wind direction uncertainty included in the datasets of large wind farms. The technique is applied to the Horns Rev offshore wind farm due to the large amount of data available. Simulations from the Jensen model,[2,3*] the Larsen model[25] and Fuga[26] are used to validate the robustness of the method in single and multiple wake situations in Section 4 with a discussion of the results. Section 5 presents the main conclusions.

2. MEASUREMENTS

The Horns Rev offshore wind farm is located in the North Sea 14 km from the west coast of Denmark. It has a total rated power capacity of 160 MW and consists of 80 pitch-controlled, variable speed Vestas V80 wind turbines (Vestas Wind Systems A/S, Hedeager 44, 8200 Aarhus N, Denmark) with a rotor diameter (D) of 80 m and a hub height of 70 m. As shown in Figure 1, the wind turbines are positioned in a regular array of 8 by 10 turbines with a spacing along the main directions of $7D$. The horizontal rows are here referred to rows A to H, whereas the vertical rows are referred to columns 1 to 10. The yaw position sensor of turbine G1 was used to determine the reference wind direction for the westerly sector

---

*Here, the Jensen model refers to the cluster wake model suggested by Katic *et al.*[3] (also known as Park) using the single wake model of Jensen[2].

$(270° \pm 65°)$ as suggested by Hansen *et al.*[22] Due to the lack of calibration of this sensor, the yaw position offset of turbine G1 was derived to ensure the maximum power ratio between G1 and G2 precisely at 270°.

The dataset represents three full years of wind farm operation (January 1, 2005 to December 31, 2007) extracted from the wind farm supervisory control and data acquisition system. The 10 min average statistics were quality controlled and processed as described by Hansen *et al.*.[22] In the current study, all atmospheric stability and turbulence conditions are included. In addition, the dataset was filtered to try to ensure flow stationarity throughout the whole wind farm. As proposed by Hansen *et al.*,[22] this filter considers only the second of two subsequent 10 min periods where both wind speed and wind direction remain within the desired flow case (e.g., 8 m s^{-1} ± 0.5 m s^{-1} and $270° \pm 2.5°$). This criterion is used to exclude periods where the wind farm is partly covered by weather fronts. It is especially restrictive for narrow wind direction sectors.

3. NUMERICAL METHODS

This section describes first the basics of the three engineering wake models used in this investigation. The method to post-process the numerical simulations and address the wind direction uncertainty is then presented.

3.1. Wake models

The Jensen model, the Larsen model and Fuga are cluster wake models that assume neutral atmospheric stability, although the Jensen and Larsen models have parameters that can be calibrated to work under a range of atmospheric conditions. The three models can compute the wake deficits of large wind farms within seconds on a personal computer and therefore can also be coupled to wind resource software to estimate the annual energy production (AEP).

3.1.1. Jensen model.

From the law of mass conservation, an expression for the wake velocity as a function of distance downstream is derived in the original Jensen model.[2] The initial velocity deficit is calculated from the turbine's thrust coefficient, and the rate of wake expansion is determined through a semi-empirical coefficient (k). The total velocity deficit for a given location is calculated as in Katic *et al.*,[3] i.e. as the square root of the sum of squares of the velocity deficits induced by all upstream turbines. In offshore conditions, it is common practice to set k to 0.05 and 0.04 for small and large wind farms, respectively. In this study, the values 0.05 and 0.04 are used for the single wake and multiple wake cases, respectively.

3.1.2. Larsen model.

The Larsen model corresponds to the most recent update of the model from Larsen.[25] The model has a closed form expression of the wake radius and wake velocity based on a simplification of the RANS equations and an empirical calibration of the wake radius at $9.6D$.[25] The velocity recovery and wake expansion are controlled by the turbine's thrust coefficient and the ambient turbulence intensity. The total velocity deficit for a given location is calculated as the linear sum of the velocity deficits induced by all upstream turbines.

A turbulence intensity of 7% is applied to the model for all flow cases investigated in this paper. This value is consistent with measurements documented by Hansen *et al.*[22] for westerly winds of 8 m s^{-1} at Horns Rev.

3.1.3. Fuga.

Fuga is a linear flow solver based on the steady-state RANS equations. It is designed for flat and homogeneous terrain so its main purpose is wake modeling of offshore wind farms. The flow is assumed incompressible and lid driven at a chosen height above the ground. The Reynolds stress tensor is modeled using a simple eddy viscosity turbulence closure. An actuator disc technique accounts for the wind turbine forcing on the flow. No numerical grid is required by the solver, which eliminates user dependence and numerical diffusion. The complete description of the model and its evaluation with wind farm datasets are found in the study of Ott *et al.*.[26]

Fuga is currently implemented as a stand-alone graphical user interface that requires a wind farm layout and wind turbine parameters in WAsP format. In this study, Fuga version 2.0.0.28 is used with a roughness length of 0.0001 m and a boundary layer height of 500 m. These values are consistent with the work from Ott *et al.*[26] and numerical simulations from the Weather Research and Forecasting model.[27]

3.2. Simulation post-processing

The wind direction uncertainty of the dataset originates from the yaw misalignment of the reference wind turbine, the spatial variability of the wind direction within the wind farm and the variability of the wind direction within the averaging

period. First, the qualitative impact of these three sources of uncertainty is described and then the post-processing technique used to address the wind direction uncertainty is presented.

3.2.1. Sources of wind direction uncertainty.

The yaw misalignment of the reference turbine is caused by the inability of the turbine control strategy to respond instantaneously to natural wind direction variations. Therefore, there is a strong correlation between the behavior of the wind direction and the measured yaw error. Figure 2 shows that a normal distribution fits well the measured wind direction variations within a 10 min period at Horns Rev. These measurements were recorded using a sonic anemometer with a sampling rate of 12 Hz at a height of 50 m.[28] Since the wind direction variations within one averaging period can be assumed to be normally distributed, the yaw error of the reference turbine can also be considered as a normally distributed random variable.

The wind direction uncertainty from spatial variability is correlated with the stochastic behavior of the wind direction. In this case, the uncertainty is caused by the difference of wind direction between the reference turbine and the other turbines in the wind farm. Ott and Longnecker[29] proved that the difference of two normally distributed variables is also normally distributed. Therefore, the wind direction uncertainty between two locations in a wind farm has a normally distributed behavior similar to the wind direction variations at the two locations. Due to spatial coherence, the amplitude of the uncertainty is expected to increase with the distance from the reference location.

Numerical simulations performed for a fixed wind direction are not fully consistent with the fact that the wind direction varies during the averaging period. It can be argued that model calibrations should partly account for the wind direction variations through the prescribed turbulence intensity and rate of wake expansion. However, the drift of the wind direction between two averaging periods is not modeled in the simulations because it corresponds to large-scale weather phenomena. Therefore, a fraction of the random behavior of the wind direction within one averaging period is not modeled and represents a wind direction uncertainty included in the dataset. This uncertainty is greatly decreased in the current study by the flow stationarity filter described in Section 2. However, it is possible that the dataset still includes non-stationary flows because, among others, the filtering process is biased by the yaw misalignment of the reference turbine.

3.2.2. Weighted average.

The method to address the wind direction uncertainty is to replace the traditional simulation performed with the 10 min average wind direction by a weighted average of several simulations covering a wide span of directions. Section 3.2.1 emphasized the fact that the wind direction uncertainty is correlated with the normally distributed behavior of the wind direction within one averaging period. Therefore, the average is applied according to the probability weight of a normal distribution centered on the desired wind direction. The weighted average is performed within ± 3 standard deviations (σ_a) to ensure a cumulative probability of 99.7%. The amplitude of σ_a is here considered as a measure of the wind direction uncertainty in the dataset.

The implementation of a weighted average does not increase the computation time significantly because the calculation for one wind direction is already very fast with the three wake models presented in Section 3.1. The wind direction resolution used to perform the simulations in the span of the weighted average is 0.5°.
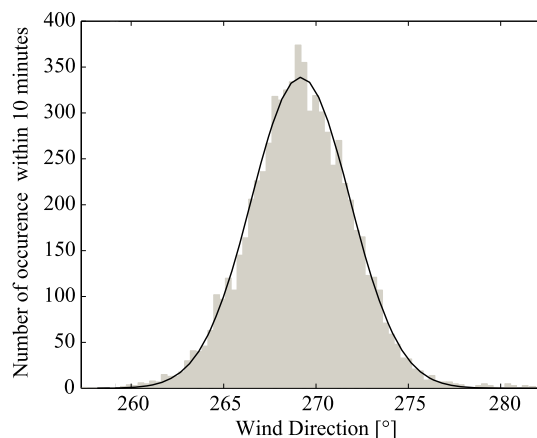
Figure 2. Measured wind direction within a 10 min period at Horns Rev using a sonic anemometer with a sampling rate of 12 Hz. The recorded turbulence intensity for the 10 min period was 5.8%. The full line represents a normal fit with a mean direction of 269.2° and a standard deviation of 2.67°.

4. RESULTS AND DISCUSSION

The results are divided into two main parts. First, the flow interaction between two wind turbines is analysed to show how the weighted average influences the shape of the power deficit in a single wake condition. Then, the power deficits along the rows of wind turbines are studied to emphasize the performance of the method for narrow and wide directional sectors.

It is worth mentioning that the datasets slightly differ in the two subsections. The single wake flow case represents the wind speed range $8\,\mathrm{m\,s^{-1}} \pm 1\,\mathrm{m\,s^{-1}}$, whereas the multiple wake cases correspond to $8\,\mathrm{m\,s^{-1}} \pm 0.5\,\mathrm{m\,s^{-1}}$. Nevertheless, all simulations were accomplished for a fixed wind speed of $8\,\mathrm{m\,s^{-1}}$.

4.1. Flow interaction between two wind turbines

Figure 3 shows the power of turbine G2 normalized to the reference turbine G1 as a function of wind directions relative to 270°. More precisely, the power of turbine G2 was normalized for each time stamp and then aggregated over the period of the data. The average sample size for each data point corresponds to 5 h of measurements with a bias for stable atmospheric conditions.[22] Similarly to previous wake modeling investigations,[6,21] the error bars included in the plots provide an indication of the scatter in the measurements by illustrating ± 0.5 standard deviation of the measured 10 min averages.

A linear moving average of 5° was applied on the results of the weighted simulations to be consistent with data processing.[22] Therefore, the weighted average on the interval $\pm 3\sigma_a$ accounts for the wind direction uncertainty included in the dataset, and the subsequent linear moving average accounts for data binning. The curves with no weighted average ($\sigma_a = 0°$) correspond to the baseline results where the wind direction uncertainty is not addressed.
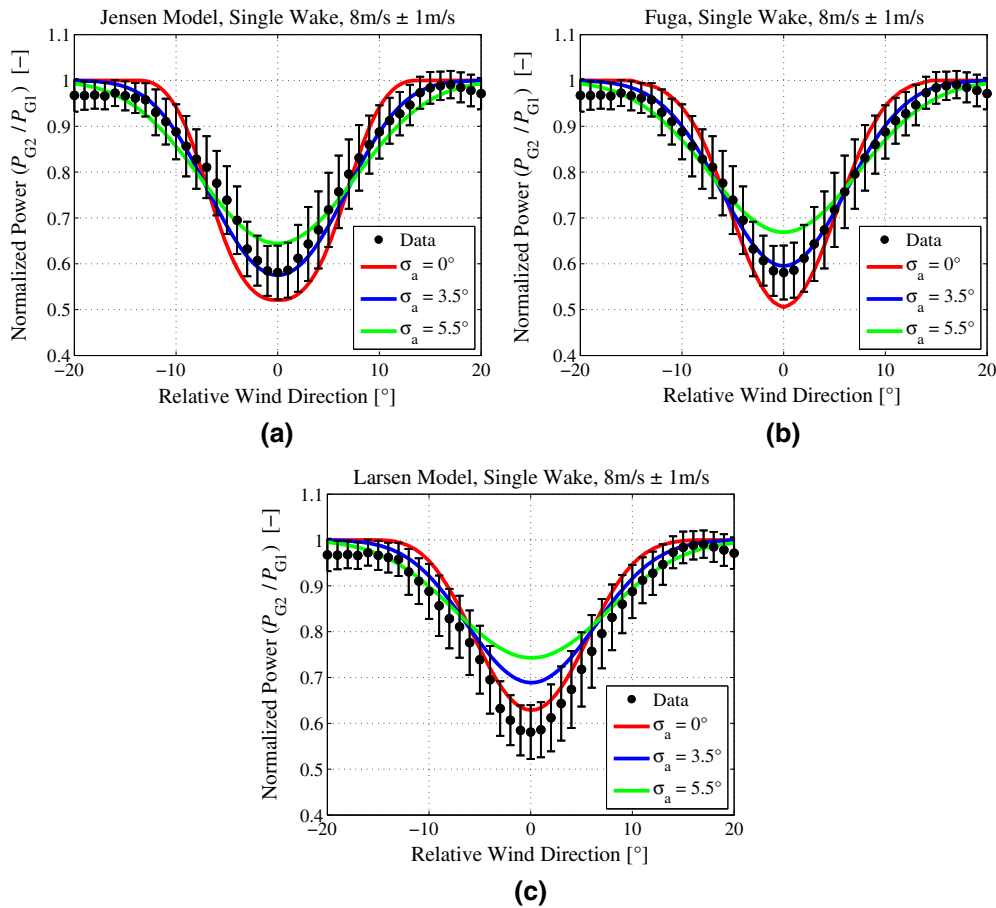
Figure 3. Influence of the weighted average on the predictions of (a) the Jensen model, (b) Fuga and (c) the Larsen model. The normalized power of turbine G2 is plotted as a function wind directions relative to 270°. The error bars correspond to ± 0.5 standard deviation of the measured normalized power.

For the three models, the normalized power simulated in the interval $[-7°,+7°]$ increases with σ_a because the weighted average includes wind directions where the turbine operates in wake free or partial wake conditions. Alternatively, the normalized power in the intervals $[-15°,-7°]$ and $[+7°,+15°]$ decreases with increasing σ_a because the weighted average includes more cases where the turbine operates in full wake condition.

The proposed method clearly improves the shape of the normalized power deficit when $\sigma_a = 3.5°$ is applied to both the Jensen model and Fuga. This value is slightly higher than the standard deviation of the wind direction for the 10 min period reported in Figure 2. This difference suggests that σ_a cannot be derived directly from the wind data. However, the amplitude of σ_a is believed to be an adequate first estimate of the wind direction uncertainty for similar turbine spacings, wind conditions and data processing methods.

It must be underlined that the Larsen model obtains better agreement in terms of the shape when no weighted average is applied. This different behavior might be caused by the empirical calibration of the model from single wake measurements at the Vindeby offshore wind farm.[25] Therefore, the calibrated shape of the normalized power deficit already includes a wind direction uncertainty. Also, the Larsen model might simply overpredict the power production in single wake conditions and fully aligned flow. Indeed, the weighted average improves the agreement of the Larsen model in the intervals $[-15°,-7°]$ and $[+7°,+15°]$, although the overall shape is mispredicted.

4.2. Power deficit along rows of wind turbines

Figure 4 presents the averaged power of each column in the wind farm normalized to the production of the reference turbine G1. The simulations and data were averaged over the wind direction sectors $270°\pm2.5°$ and $270°\pm15°$ in Figure 4(a) and (b), respectively. The average sample size for each data point corresponds to 7 h 40 min for the $\pm2.5°$ sector and 757 h for the $\pm15°$ sector. The two plots include no weighted average on the simulations to present the baseline performance of the models.

The three models significantly underpredict the power production for the narrow sector ($\pm2.5°$), while obtaining good to excellent results for the wide sector ($\pm15°$). The correlation between the span of the sector and the accuracy of the wake models was underlined by Gaumond *et al.*[23] and documented in previous studies.[10,24] Due to the wind direction uncertainty described in Section 3.2.1, narrow wind direction sectors of 5° most likely include situations where the turbines operate in conditions outside the span of the sector. This means that the turbines operate more often in wake free or partial wake situations (i.e., higher power outputs) than what is modeled by the numerical simulations. In turn, when the sector width increases the wind direction uncertainty becomes less significant and less cases are filtered in the wrong bins. The agreement in Figure 4(b) is therefore improved because the simulations for wider sectors are more representative of the datasets.

A further investigation of the power production of the individual rows shows that a lateral power gradient exists. Figure 5(a) illustrates the normalized power of rows A, B, E, F and G. The power clearly increases from rows G to A (the normalized power of rows C, D and H is not shown for clarity reasons, but the increasing trend as a function of distance from row G is applicable to all rows[30]). It is worth mentioning that the power of turbine G2 in Figure 5(a) differs
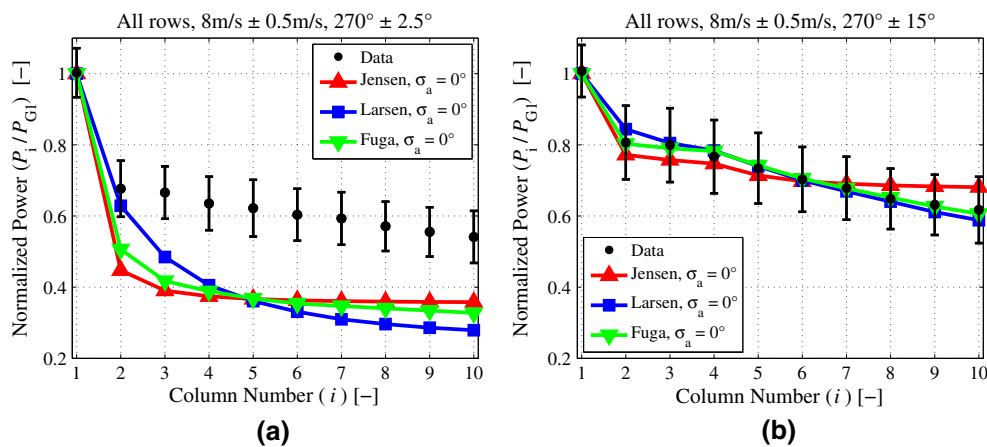
Figure 4. Average power of each column of the wind farm (all rows included) normalized to the production of the reference turbine G1 for two different averaging sectors: (a) $270° \pm 2.5°$ and (b) $270° \pm 15°$. No weighted average was applied on the simulations. The error bars correspond to $\pm$ 0.5 standard deviation of the measured power production.

from the power with a relative wind direction of 0° in Figure 3 due to the different wind speed range used in the filtering process. In fact, the results from Hansen *et al.*[22] suggest that Figures 4 and 5(a) represent atmospheric conditions that are less stable than Figure 3.

The results in Figure 5(a) do not necessarily imply that row A generated more power than rows B, E and F, which in turn had a higher power output than row G. In fact, the lateral power gradient is an indication that the estimation of the wind direction is less accurate when the distance from the rows to the reference turbine G1 increases. A less accurate estimation of the wind direction yields more cases that are wrongly filtered in the narrow bin $270° \pm 2.5°$. These misfiltered cases correspond to wake free or partial wake situations that increase artificially the power in the rows. Therefore, the lateral power gradient is an artifact of the data processing resulting from the increasing wind direction uncertainty. This aspect should be considered when comparing numerical simulations with power production data because the evaluation of the wake models might vary depending on which row or group of rows is selected for the comparison. With the lowest wind direction uncertainty, row G has probably the most representative behavior of the real power production for the narrow wind direction sector $270° \pm 2.5°$.

Figure 5(b) illustrates the normalized power of the turbines located in the second column of the wind farm. It can be seen that the power increases almost linearly from G2 to A2. This result shows that the wind direction uncertainty increases linearly with the distance perpendicular to the mean wind direction. This uncertainty is significant because turbine A2 produces 14% more power than G2 for the same wind direction sector. To account for the uncertainty from spatial variability of the wind direction, the simulations from Fuga are fitted to the data of column 2 in Figure 5(b) using a row-specific σ_a value. Fuga is here used because it is the most accurate model for the wide sector (Figure 4(b)), where the uncertainty is assumed negligible. Fitting the simulations from Fuga for the narrow sector therefore provides the most accurate estimate of the uncertainty. These values are presented in Table I, where it is observed that σ_a increases proportionally to the distance from row G where the reference turbine is located.

Figure 6 shows the results when the weighted average technique is applied to the simulations using the row-specific σ_a from Table I. The results for the narrow sector in Figure 6(a) are significantly improved compared with those in Figure 4(a). Interestingly, the fitted row-specific σ_a for the second turbine in each row also improves the agreement of the remaining turbines in the rows. The apparent absence of an increased uncertainty along the rows is consistent with the stationary flow filter that intends to ensure uniform downstream conditions. As underlined by Gaumond *et al.*[23] for the Lillgrund offshore wind farm, an increasing wind direction uncertainty along the rows is possible when the dataset is processed with a short averaging period and the absence of a stationary flow filter.

The accuracy of the three models for the wide sector $270° \pm 15°$ remains almost unchanged when using the row-specific σ_a (Figure 6(b)) compared with the results for $\sigma_a = 0°$ (Figure 4(b)). This outcome shows that the weighted average methodology based on the normal probability distribution is a robust tool to address the wind direction uncertainty because it does
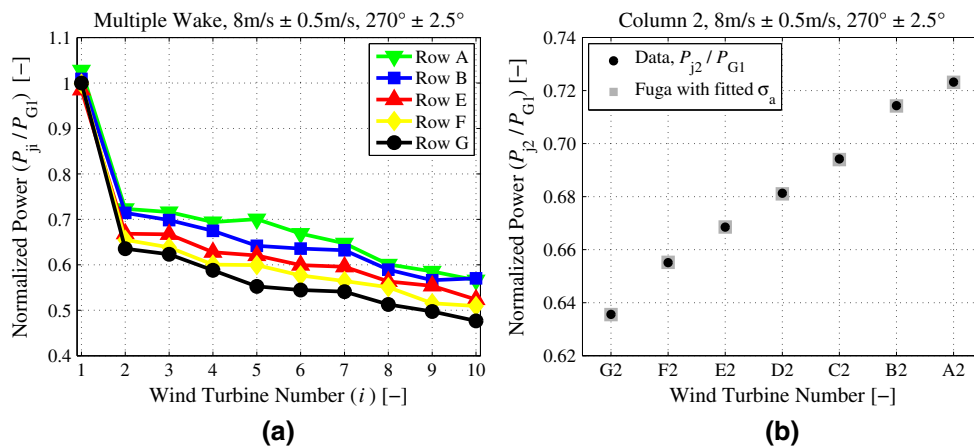
Figure 5. (a) Power production data of rows A, B, E, F and G normalized to the reference turbine G1 for the sector $270° \pm 2.5°$. (b) Normalized power of the second turbine in rows A to G for the sector $270° \pm 2.5°$. The fitted values of σ_a from Fuga are in Table I.

Table I. Fitted σ_a values to the normalized power of the second turbine in each row for the sector $270° \pm 2.5°$.

Turbine number	A2	B2	C2	D2	E2	F2	G2	H2
Fitted σ_a with Fuga	7.4°	7.0°	6.2°	5.8°	5.4°	5.0°	4.5°	4.8°
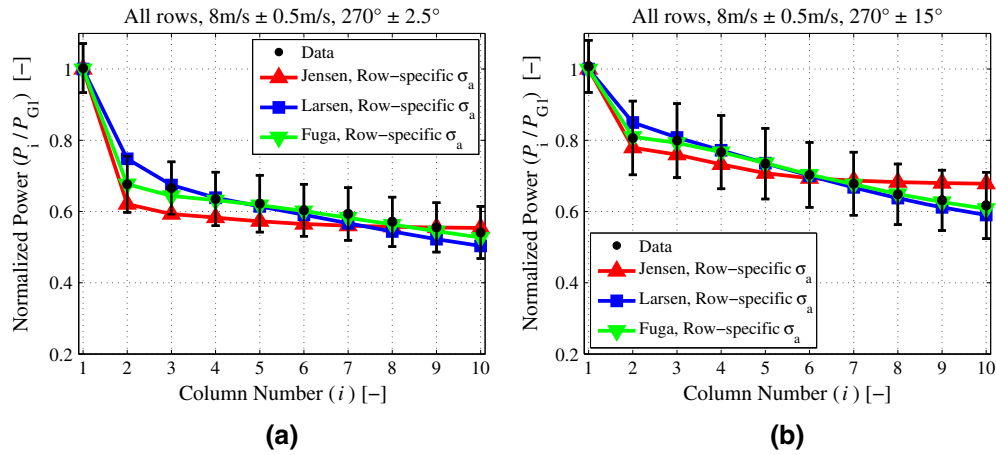
Figure 6. Average power of each column of the wind farm (all rows included) normalized to the production of the reference turbine G1 for two different averaging sectors: (a) 270° ± 2.5° and (b) 270° ± 15°. The weighted average was applied on the simulations using the row-specific σ_a from Table I. The error bars correspond to ± 0.5 standard deviation of the measured normalized power.

not alter the performance of the wake models. As mentioned in Section 4.1 for the single wake situation, the weighted average technique also improves the shape of the power deficit, which results in a better agreement for both the narrow and wide directional sectors in multiple wake situations.

Table II shows the results of the efficiency of the Horns Rev wind farm with all wind turbines operating. The simulations with $\sigma_a = 0°$ correspond to the baseline results where the wind direction uncertainty is not addressed. The results confirm that the wake models predict accurately the power production of the wind farm for the averaging sector $270° \pm 15°$ independently of the method used. However, the proposed weighted average technique improves the agreement of the simulations for the narrow sector to a 1% margin with the Larsen model and Fuga.

Two potential applications of the method are wind farm control algorithm and layout optimization because they require accurate predictions for narrow wind direction sectors. However, post-processing technique does not seem to be highly valuable for the computation of the AEP because in this case the simulations are commonly averaged over wind direction sectors of 30°.

It is worth mentioning that although the three models accurately predict the efficiency of the wind farm for the wide sector in Table II, the Larsen model and Fuga capture more accurately the reduction of power along the rows in Figures 4(b) and 6(b). Alternatively, the high accuracy of the Jensen model (+0.1%) is caused by balancing errors from the underprediction of the first five columns and the overprediction of the last four ones. If the number of columns in each row was higher, the Larsen model and Fuga would potentially still make accurate power predictions of the last turbines in the rows, whereas the Jensen model would probably overpredict their power. This is an important aspect to consider when predicting wakes with such models because the size of future wind farms will likely increase. The overprediction of the Jensen model can however be mitigated by reducing the value of k for deeper turbines in the array.[31]

Our results indicate that the discrepancies between the traditional numerical simulations and power production data for narrow wind direction sectors are not caused by an inherent inaccuracy of the engineering wake models, but rather by a large wind direction uncertainty included in the dataset. Therefore, modifying the wake model parameters to fit specific measurements for narrow sectors[10,19] is a risky approach that might deteriorate AEP predictions based on wide sectors.

Table II. Efficiency of the Horns Rev wind farm at 8 m s^{-1} ± 0.5 m s^{-1}.

Averaging sector	270°± 2.5°	270°± 15°
Measured wind farm efficiency	64.7%	73.9%
Jensen model with $\sigma_a = 0°$	−20.9%	+0.4%
Larsen model with $\sigma_a = 0°$	−20.9%	−0.1%
Fuga with $\sigma_a = 0°$	−21.7%	−0.3%
Jensen with row-specific σ_a	−3.1%	+0.1%
Larsen with row-specific σ_a	−0.7%	−0.2%
Fuga with row-specific σ_a	−0.8%	−0.2%

In addition, this kind of calibration includes the specific dataset uncertainty, which might not be applicable to another wind farm. Figure 5(a) clearly illustrates that even within the same wind farm, the choice of row would influence the model calibration.

5. CONCLUSION

A method to address the wind direction uncertainty included in the dataset of the Horns Rev offshore wind farm is presented. The method replaces the traditional simulations performed with the 10 min average wind direction by a weighted average of several simulations covering a wide span of directions. The weighted average is based on a normal probability distribution to account for the uncertainty from the yaw misalignment of the reference turbine, the spatial variability of the wind direction inside the wind farm and the variability of the wind direction within the averaging period.

The results show that the post-processing technique improves the agreement of the simulations for single and multiple wake cases. The shape of the power deficit is more consistent with the dataset, and the underpredictions of the models for narrow wind direction sectors are significantly improved. The robustness of the method is verified using three different wake models, namely the Jensen model, the Larsen model and Fuga. The results show that the discrepancies between the results of numerical simulations and power production data for narrow wind direction sectors in previous studies[10,12,23,24] were not caused by an inherent inaccuracy of the models, but rather by a large wind direction uncertainty in the dataset.

Future work shall verify if the proposed method can consistently improve the simulation results at other large wind farms. In addition, further investigations should attempt to quantify the wind direction uncertainty independently of the wake models applied. It would be interesting to establish a correlation between the standard deviation of the wind direction within the averaging period and the value of σ_a.

ACKNOWLEDGEMENTS

REFERENCES

1. Barthelmie RJ, Hansen K, Frandsen ST, Rathmann O, Schepers JG, Schlez W, Phillips J, Rados K, Zervos A, Politis ES, Chaviaropoulos PK. Modelling and measuring flow and wind turbine wakes in large wind farms offshore. *Wind Energy* 2009; **12**: 431–444.

2. Jensen NO. A note on wind generator interaction. *Technical Report Risø-M-2411*, Risø National Laboratory, Roskilde, 1983.

3. Katic I, Højstrup J, Jensen NO. A simple model for cluster efficiency, *Proceedings of the European Wind Energy Association Conference*, Rome, 1986; 407–410.

4. Ainslie JF. Calculating the flowfield in the wake of wind turbines. *Journal of Wind Engineering and Industrial Aerodynamics* 1988; **27**: 213–224.

5. Schlez W, Neubert A. New developments in large wind farm modelling, *Proceedings of the European Wind Energy Association Conference*, Marseille, 2009.

6. Barthelmie RJ, Jensen LE. Evaluation of wind farm efficiency and wind turbine wakes at the Nysted offshore wind farm. *Wind Energy* 2010; **13**: 573–586.

7. Frandsen S, Barthelmie R, Pryor S, Rathmann O, Larsen S, Højstrup J, Thøgersen M. Analytical modelling of wind speed deficit in large offshore wind farms. *Wind Energy* 2006; **9**: 39–53.

8. Frandsen ST, Jørgensen HE, Barthelmie R, Rathmann O, Badger J, Hansen K, Ott S, Rethore PE, Larsen SE, Jensen LE. The making of a second-generation wind farm efficiency model complex. *Wind Energy* 2009; **12**: 445–458.

9. Sanderse B, Pijl SP, Koren B. Review of computational fluid dynamics for wind turbine wake aerodynamics. *Wind Energy* 2011; **14**: 799–819.

10. Garza J, Blatt A, Gandoin R, Hui SY. Evaluation of two novel wake models in offshore wind farms, *Proceedings of the European Wind Energy Association Offshore Conference*, Amsterdam, 2011.

11. Montavon C, Hui SY, Graham J, Malins D, Housley P, Dahl E, Villiers P, Gribben B. Offshore wind accelerator: wake modelling using CFD, *Proceedings of the European Wind Energy Association Conference*, Brussels, 2011.

12. Ivanell S, Mikkelsen RF, Sørensen JN, Hansen KS, Henningson D. The impact of wind direction in atmospheric BL on interacting wakes at Horns Rev wind farm, *Proceedings of the Science of Making Torque from Wind Conference*, Heraklion, 2010; 407–426.

13. Troldborg N, Sørensen JN, Mikkelsen R. Numerical simulations of wake characteristics of a wind turbine in uniform inflow. *Wind Energy* 2010; **13**: 86–99.

14. Troldborg N, Larsen GC, Madsen HA, Hansen KS, Sørensen JN, Mikkelsen R. Numerical simulations of wake interaction between two wind turbines at various inflow conditions. *Wind Energy* 2011; **14**: 859–876.

15. Churchfield MJ, Lee S, Moriarty PJ, Martinez LA, Leonardi S, Vijayakumar G, Brasseur JG. A large-eddy simulation of wind-plant aerodynamics, *50th American Institute of Aeronautics and Astronautics Meeting*, Nashville, TN, 2012; 1–19.

16. El Kasmi A, Masson C. An extended $k - \epsilon$ model for turbulent flow through horizontal-axis wind turbines. *Journal of Wind Engineering and Industrial Aerodynamics* 2008; **96**: 103–122.

17. Réthoré PE, Sørensen NN, Bechmann A, Zhale F. Study of the atmospheric wake turbulence of a CFD actuator disc model, *Proceedings of the European Wind Energy Association Conference*, Marseille, 2009.

18. Réthoré PE, Sørensen NN, Bechmann A. Modelling issues with wind turbine wake and atmospheric turbulence, *Proceedings of the Science of Making Torque from Wind Conference*, Heraklion, 2010; 349–357.

19. Rados KG, Prospathopoulos JM, Stefanatos NC, Politis ES, Chaviaropoulos PK, Zervos A. CFD modeling issues of wind turbine wakes under stable atmospheric conditions, *Proceedings of the European Wind Energy Association Conference*, Marseille, 2009.

20. Phillips JL, Cox SD, Henderson AR, Gill JP. Wake effects within and between large wind projects: the challenge of scale, density and neighbours – onshore and offshore, *Proceedings of the European Wind Energy Association Conference*, Warsaw, 2010.

21. Barthelmie RJ, Pryor SC, Frandsen ST, Hansen KS, Schepers JG, Rados K, Schlez W, Neubert A, Jensen LE, Neckelmann S. Quantifying the impact of wind turbine wakes on power output at offshore wind farms. *Journal of Atmospheric and Oceanic Technology* 2010; **27**: 1302–1317.

22. Hansen KS, Barthelmie RJ, Jensen LE, Sommer A. The impact of turbulence intensity and atmospheric stability on power deficits due to wind turbine wake at Horns Rev wind farm. *Wind Energy* 2012; **15**: 183–196.

23. Gaumond M, Réthoré PE, Bechmann A, Ott S, Larsen GC, Peña A, Hansen KS. Benchmarking of wind turbine wake models in large offshore wind farms, *Proceedings of the Science of Making Torque from Wind Conference*, Oldenburg, 2012.

24. Beaucage P, Robinson N, Brower M, Alonge C. Overview of six commerical and research wake models for large offshore wind farms, *Proceedings of the European Wind Energy Association Conference*, Copenhagen, 2012; 95–99.

25. Larsen GC. A simple stationary semi-analytical wake model. *Technical Report Risø-R-1713(EN)*, Risø National Laboratory, Roskilde, 2009.

26. Ott S, Berg J, Nielsen M. Linearised CFD models for wakes. *Technical Report Risø-R-1772(EN)*, Risø National Laboratory, Roskilde, 2011.

27. Peña A, Gryning SE, Hahmann AN. Observations of the atmospheric boundary layer height under marine upstream flow conditions at a coastal site. *Journal of Geophysical Research* 2013; **118**: 1924–1940. DOI: 10.1002/jgrd.50175.

28. Peña A, Hahmann AN. Atmospheric stability and turbulence fluxes at Horns Rev - an intercomparison of sonic, bulk and WRF model data. *Wind Energy* 2012; **15**: 717–731.

29. Ott RL, Longnecker M. *An Introduction to Statistical Methods and Data Analysis*, (6 edn). Brooks/Cole, Cengage Learning: Belmont, California, 2010.

30. Hansen KS, Barthelmie R, Jensen LE, Sommer A. Power deficits due to wind turbine wakes at Horns Rev wind farm, *Proceedings of the Science of Making Torque from Wind Conference*, 2010; 40–46.

31. Peña A, Rathmann O. Atmospheric stability dependent infinite wind farm models and the wake decay coefficient. *Wind Energy* 2012.